Hindawi
Advances in OptoElectronics
Volume 2019, Article ID 2938652, 6 pages
https://doi.org/10.1155/2019/2938652

Research Article

Impact of the Four-Sideband and Two-Sideband Theories in Designing of Fiber Optical Parametric Amplifiers

Kumbirayi Nyachionjeka,[1] **Hillary Tarus**,[2] **and Philip Kibet Langat**[3]

[1]*Department of Electrical Engineering, Pan African University Institute of Science Technology and Innovation, Juja, Kenya*
[2]*Directorate of Operations, West Indian Ocean Cable Company (WIOCC), Nairobi, Kenya*
[3]*Department of Telecommunications and Information Technology Engineering, Jomo Kenyatta University of Agriculture and Technology, Juja, Kenya*

Correspondence should be addressed to Kumbirayi Nyachionjeka; kuuh29@gmail.com

Received 31 May 2019; Revised 1 August 2019; Accepted 11 September 2019; Published 7 October 2019

Academic Editor: Jung Y. Huang

In this paper, we seek to compare the two design theories for fiber optical parametric amplifier through simulation. The two-sideband method (standard method) has been the most widely used method in fiber optical parametric amplifier design, but it does not predict the gain shrinkage around the pumps. This technique does not consider the gain shrinking dynamics around the pump(s). The four-sideband analytical technique is an alternative technique for fiber optical parametric amplifier design, and it allows for a simplified investigation of the gain shrinking dynamics around the pump(s) due to the interaction of the various arising high-order idlers within the vicinity of the pump waves. The undertaking in this paper is to present a dual-pump fiber amplifier based on the highly nonlinear fiber and another one based on the photonic crystal fiber and ascertain if gain shrinking affects both FOPAs.

1. Introduction

The adoption of the fiber optical parametric amplifier (FOPA) in telecommunications will go a long way in enabling broadband and quality internet. The research in this area has undergone phenomenal progression in the last few years as researchers seek an alternative amplifier to compete with the traditional optical amplifiers which are limited in their bandwidth and have unstable gain dynamics due to their material composition [1]. The imminent launching of 5G around the world has made it even more important to have amplifiers that can enable broadband communications and increase the reach of fiber networks while reducing costs [2]. The many functions that come with FOPA have made it a front contender as a future amplifier in passive optical networks (PONs). The FOPA can be used in many applications such as ultrafast signal processors and optical wavelength converters; FOPAs utilize the four-wave mixing (FWM) in which the amplifying waveguide dispersion is designed such that an effective transfer of energy occurs between one or two pump waves, signal, and a generated idler wave [3, 4]. The dual-pump FOPA can be arranged in such a way that the pumps are modulated out of phase. This arrangement of using out-of-phase modulated pumps allows for the reduction of pump depletion due to stimulated Brillouin scattering, and at the same time, it cancels signal gain distortion or idler spectral broadening [5]. The FWM allows for optimized placement of the two pumps so that maximum flat gain can be attained [6].

In recent times, FOPAs based on FWM and six-wave mixing with bandwidth up to 600 nm and 150 nm, respectively, have been shown [7]. Using the FWM theory, the gain bandwidth and the uniformity of parametric amplifiers can be increased significantly especially by using dual pumps. It is worth noting that the FWM principle is incomplete and hence presents an unclear and incomplete picture of the gain spectrum estimation, especially when the signal is placed close to one of the pumps. Four-sideband

waves are birthed by two processes, that is, the Bragg scattering and the modulation instability, and these resonantly interact with one another leading to a process called gain shrinking around the pump(s) [3, 8]. When the pump is placed very close to one of the pumps, modulation instability (MI) becomes the dominant process and is then used to define the resulting interactions. Radic and McKinstrie investigated the concept of four sidebands by using two pumps separated by 25 nm, and the signal was placed 0.9 THz from the average pump frequency, and in their experiment, they determined the existence of high idlers when a signal is in the vicinity of the pump [9]. In [10], Richter et al. demonstrated a two-pump FOPA placed symmetrically around the signal in the first case, and in the second scenario, the signal and idler were placed symmetrically around one of the pumps. The emphasis was on the influence of the phase of each individual wave on the gain, and they determined that the signal and idler output power depended on the relative phases of each of the six interacting waves. Bogris et al. placed two pumps at 1530 nm and 1590 nm with the signal placed at 1554 nm, 6 nm from the average pump wavelength of 1560 nm. It was concluded that the analytical and the numerical method differed around the pumps' spectral area, and a flat gain bandwidth of 40 nm was achieved [11]. A number of two-pump FOPA designs were theoretically and experimentally demonstrated by Chavez Boggio et al., as they investigated the gain ripples in the flat gain spectrum. It was noted that ripples were affected by the length of the fiber and the fourth-order dispersion coefficient and also that the area near the pumps should be avoided when using a two-pump FOPA with a signal placed near the pumps because of the crosstalk [12].

In this paper, we set out to develop an analytical model that emphasizes on linear wave-vector mismatches to explain how the sideband and its closest pump interact. Dispersion parameters have a greater role in how the interaction between idlers and pump occurs, and thus modelling around them leads to a more accurate analytical technique. Subsequently, two dual-pump FOPAs based on highly nonlinear fibers (HNLFs) and photonic crystal fibers (PCFs) are designed using the two-sideband theory and the four-sideband theory. The photonic crystal fiber and data used for FOPA design in this paper are similar to the data used by Taghizadeh et al. in [13]. It will be shown that the four-sideband theory allows the prediction of gain shrinkage around the pumps making it appropriate for use in the designing of FOPA [7].

2. Theory and Analysis

The gain of a two-pump FOPA is obtained by solving the nonlinear Schrodinger equation with two high pump powers at frequencies, ω_2, and signal frequency at ω_3. Both the pumps are considered to be undepleted corresponding to the linear gain regime. The four-sideband interaction shown in Figure 1 can be summed up in terms of three FWM processes which are modulation interaction (MI), Bragg scattering, and phase conjugation (PC). Six continuous waves can be considered to be propagating along the fiber, i.e., pump 1, pump 2, signal, idler, sideband 1, and sideband 2. The waves have angular frequencies denoted by $\omega_1, \omega_2, \omega_3, \omega_4, \omega_5$, and ω_6, respectively.

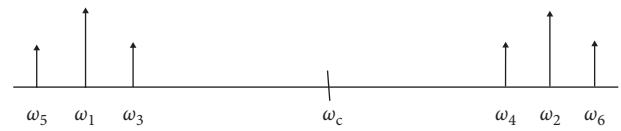

Figure 1: Dual-pump fiber FOPA process based on the six-wave model.

When two pump wavelengths are placed symmetrically about the zero dispersion wavelength ω_0 and sufficiently placed far apart, the gain bandwidth is maximized. The two-sideband process is phase matched for a signal wave placed between the pump frequencies, and an idler is generated. In such circumstances, the dual-pump FOPA is considered to be a two-sideband system. Hence, under these conditions, the four waves carry much of the power over the whole length of the fiber. The other higher-order waves arising from the FWM are badly phase matched, and they remain negligible and thus are not considered.

If the signal is placed close to any of the pumps, secondary waves are generated. Some of these secondary waves may become phase matched and may attain levels similar to levels of the signal and idler. In such situations, to get a complete description of the dynamics, these new higher-order waves are considered as they have a bearing on the gain characteristics of the FOPA. This situation happens when a two-pump FOPA's signal frequency is placed close to one of the pumps. This gives rise to two other new waves, which are placed at ω_5 and ω_6. The origins of these waves can be explained as follows. When the signal frequency is placed approximately within 10 nm of pump 1, wave, ω_5, is generated due to efficient FWM between the signal frequency and pump 1; this new wave is symmetrically placed relative to the pump, and in turn, we obtain $\omega_3 + \omega_5 = 2\omega_1$. If idler 1 is near pump 2, ω_6 which is symmetric to pump 2 is generated due to efficient FWM between idler 1 and pump 2, and this interaction is denoted by $\omega_4 + \omega_6 = 2\omega_2$. Due to these very close couplings, when a signal is near the pump, the signal grows at the same time with the three idlers, having similar gains. Hence, these higher-order idlers lead to reduction in the gain.

Firstly, when a signal frequency is located between these symmetrically placed pumps, this results in a phase-matched PC process and an idler of frequency $\omega_4 = \omega_1 + \omega_2 + \omega_3$. In such a case, the amplifier is dominated by the two-sideband theory denoted in Figure 2.

The gain of the PC (two-sideband) as shown in (2) and (3) for the idlers ω_3 and ω_4 is obtained from solving equations (1) and (2):

$$-j\frac{\partial A_3^*}{\partial z} = \left(-\Delta\beta_3 - \gamma P_1\right)A_3^* - 2\gamma\sqrt{P_1P_2}A_4, \tag{1}$$

$$-j\frac{\partial A_4}{\partial z} = 2\gamma\sqrt{P_1P_2}A_3^* + \left(\Delta\beta_4 + \gamma P_2\right)A_4. \tag{2}$$

Solving equations (1) and (2) as shown in Section A1.2 of [14] gives the gain as

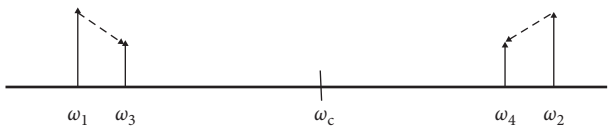

Figure 2: Dual-pump fiber FOPA process based on the four-wave model.

$$G = \frac{r^2 \cosh^2(gz)}{g^2} - \frac{4g^2}{\mathrm{K}^2}, \tag{3}$$

where K is the wave number total for all the interacting four waves as shown in (5):

$$\mathrm{K} = \gamma(P_1 + P_2) + \sum_{l}^{\infty} \frac{\beta_{2l}}{(2l)!}\left(\Delta\omega_{s1}^{2l} - \Delta\omega_p^{2l}\right), \tag{4}$$

where β_l are the dispersion related parameters that account for all dispersion-associated behaviors defined in equations (10)–(13), while $g = \sqrt{r^2 - (\mathrm{K}/2)^2}$, $r = 2\gamma\sqrt{P_1 P_2}$, $\Delta\omega_p = (\omega_2 - \omega_1)/2$, $\Delta\omega_{s1} = \Delta\omega_3 = |\omega_3 - \omega_c|$, and center frequency $\omega_c = (\omega_1 + \omega_2)/2$.

Considering (1) and (2), the following matrix can be easily obtained:

$$-j\frac{\partial}{\partial z}\begin{pmatrix} A_3^* \\ \\ A_4 \end{pmatrix} = \begin{pmatrix} -\Delta\beta_3 - \gamma P_1 & -r \\ \\ r & \beta_4 - \gamma P_2 \end{pmatrix}\begin{pmatrix} A_3^* \\ \\ A_4 \end{pmatrix}. \tag{5}$$

Equation (5) is known as the two-sideband model and is of the form $\partial X/\partial z = iNX$, with the solutions shown as $X(z) = \exp(iNz)X(0)$, where P_1 and P_2 are the pump powers and γ is the fiber nonlinearity coefficient. The linear wave mismatches are shown by $\Delta\beta_l$, where $l = 3, 4$ as in equations (10) and (11).

The conditions under which these frequencies interact in FWM is depicted as $\omega_1 + \omega_2 = \omega_4 + \omega_3$, where ω_1 and ω_2 are used as pumps and ω_3 and ω_4 are signal and idler and can be represented diagrammatically as in Figure 2.

Secondly, the waves interact differently for a six-wave arrangement (four-sideband) as shown in Figure 1. The interaction is as follows: $\omega_5 = 2\omega_1 - \omega_3$ and $\omega_6 = 2\omega_2 - \omega_4$. The center frequency ω_c is in a manner that allows the following to be possible: $2\omega_c = \omega_1 + \omega_2 = \omega_3 + \omega_4 = \omega_5 + \omega_6$. The sideband ω_6 is due to pump frequency ω_2, while sideband ω_5 is due to pump frequency ω_1, and ω_5 and ω_6 are thus the sidebands.

Pump 1, pump 2, idler, and signal are represented by A_1, A_2, A_3, and A_4 complex amplitudes, respectively. Linear wave-vector mismatch is given by $\Delta\beta$ for the PCF and HNLF, and z is the distance from the beginning of each fiber.

The arrangement of the system under simulation is such that the signal frequency is close to one of the pumps. The BS and MI also become phase matched, and the conversion efficiencies of the idlers ω_3 and ω_4 are increased. The four-sideband theory ensues and describes the interaction of the two extra-high-order idler waves that arise when the signal is near one of the pumps [3]. This phenomenon is best described and modelled by (6)–(9), assuming the pumps are not depleted:

$$\begin{aligned} -j\frac{\partial A_5}{\partial z} &= (\Delta\beta_5 + \gamma P_1)A_5 + \gamma P_1 A_3^* \\ &\quad + 2\gamma\sqrt{P_1 P_2}A_4 + 2\gamma\sqrt{P_1 P_2}A_6^*, \end{aligned} \tag{6}$$

$$\begin{aligned} -j\frac{\partial A_3^*}{\partial z} &= -\gamma P_1 A_5 + (-\Delta\beta_3 - \gamma P_1)A_3^* \\ &\quad - 2\gamma\sqrt{P_1 P_2}A_4 - 2\gamma\sqrt{P_1 P_2}A_6^*, \end{aligned} \tag{7}$$

$$\begin{aligned} -j\frac{\partial A_4}{\partial z} &= 2\gamma\sqrt{P_1 P_2}A_5 + 2\gamma\sqrt{P_1 P_2}A_3^* \\ &\quad + (\Delta\beta_4 + \gamma P_2)A_4 + \gamma P_2 A_6^*, \end{aligned} \tag{8}$$

$$\begin{aligned} -j\frac{\partial A_6^*}{\partial z} &= -2\gamma\sqrt{P_1 P_2}A_5 - 2\gamma\sqrt{P_1 P_2}A_3^* \\ &\quad - \gamma P_2 A_4 + (-\Delta\beta_6 - \gamma P_2)A_6^*, \end{aligned} \tag{9}$$

where $\Delta\beta_i$ are the linear wave mismatches which can be gathered into a matrix N as in (5) and $i = 3, 4, 5, 6$. The linear wave mismatches give an insight into the interaction of the pump and the idler nearest to it. When evaluated near ω_c using the Taylor series, the linear wave mismatches can be realized as shown in the following equations:

$$\Delta\beta_3 = \sum_{l=2}^{4} (-1)^{l*3}\frac{\beta_l}{l!}\left(\Delta\omega_3^l - \Delta\omega_p^l\right), \tag{10}$$

$$\Delta\beta_4 = \sum_{l=2}^{4} (-1)^{l*4}\frac{\beta_l}{l!}\left(\Delta\omega_4^l - \Delta\omega_p^l\right), \tag{11}$$

$$\Delta\beta_5 = \sum_{l=2}^{4} (-1)^{l*5}\frac{\beta_l}{l!}\left(\omega_5^l - \Delta\omega_p^l\right), \tag{12}$$

$$\Delta\beta_6 = \sum_{l=2}^{4} (-1)^{l*6}\frac{\beta_l}{l!}\left(\Delta\omega_6^l - \Delta\omega_p^l\right), \tag{13}$$

where $\Delta\omega_{s2} = \Delta\omega_4 = |\omega_4 - \omega_c|$, $\Delta\omega_5 = 2\Delta\omega_p - \Delta\omega_{s1}$, and $\Delta\omega_6 = 2\Delta\omega_p - \Delta\omega_{s2}$. Equations (6)–(9) can be written as $\partial X/\partial z = iNX$ with the solutions shown as $X(z) = \exp(iNz)X(0)$.

3. Methodology and Results

In this research, we set out to investigate the merits, demerits, and impact of two theories by designing FOPA based on each theory. The main aim was to investigate the behavior of the gain around each pump when a signal wave is placed within 10 nm of the pump(s) wave. The two-sideband theory has been extensively researched and has led to many breakthroughs in the area of FOPA. To achieve

the aim, two prominent materials used in the design of FOPA were selected for simulation and design of FOPA, i.e., the traditional HNLF with a relatively low nonlinear coefficient and the new material PCF with a very high nonlinear coefficient. For the HNLF, two amplifiers were simulated, one based on the two-sideband theory and the other on the four-sideband theory, and the resulting gain spectrums were analyzed; similarly, the same simulation setup was done for the PCF. In all designs, the signal frequency was placed near one of the pumps, i.e., within 10 nm, and this allows for the investigation of the effects of BS and MI on pump performance. The pump separation was below 100 nm for all the simulations.

Equations (6)–(9) were numerically solved and simulated in MATLAB using the in-built exponential matrix operator. Independent solutions to the N matrix were found, and a FOPA was achieved for a phase insensitive design; the initial conditions for the amplitude were set at $[0\ 1\ 0\ 0]^{T}$. It is adequate to consider only β_2, β_3, and β_4 values as these are the reason for all the behaviors that are dispersion related. The parametric gain simulation was done for the signals between $[\omega_1 - \Delta\omega_p \omega_2 + \Delta\omega_p]$.

The first design was based on the standard two-sideband theory. To achieve the design, the following parameters were used: length = 243 m, $\beta_2 = 6.4 \times 10^{-30}$ ps^2·km^{-1}, $\beta_3 = 0.65 \times 10^{-41}$ ps^3·km^{-1}, $\beta_4 = -1.65 \times 10^{-55}$ ps^4·km^{-1}, $P_1 = 1.9$ W, $P_2 = 1.3$ W, $\gamma = 8$ W^{-1}·km^{-1}, $\lambda_1 = 1522$ nm, and $\lambda_2 = 1603$ nm.

Equation (5) was simulated and the following graph was obtained. The graph is what is typically obtained for the standard FWM model. The flat gain obtained for this amplifier design is 36 dB over a gain bandwidth of 32 nm as shown in Figure 3.

The same parameters as above were used in simulating a four-sideband design: length = 243 m, $\beta_2 = 6.4 \times 10^{-30}$ ps^2·km^{-1}, $\beta_3 = 0.65 \times 10^{-41}$ ps^3·km^{-1}, $\beta_4 = -1.65 \times 10^{-55}$ ps^4·km^{-1}, $P_1 = 1.9$ W, $P_2 = 1.3$ W, and $\gamma = 8$ W^{-1}·km^{-1}. For the four-sideband theory, a FOPA was designed as shown in Figure 4. The gain and gain bandwidth achieved with the HNL fiber was 36 dB and 32 nm, respectively, when modelled using the four-sideband theory.

Extending the four- and two-sideband theory models to FOPA designs based on PCFs, Figures 5 and 6 depict the gain profiles, respectively. Because of the high nonlinearity coefficient, the gain and bandwidth of the FOPA increase when compared to HNLFs.

In [13], a single pulsed-pump FOPA based on the PCF was demonstrated. Adopting the parameters that were realized from the PCF design, we were able to simulate a dual-pump FOPA using the two-sideband and the four-sideband theories. The parameters used were as follows: length = 35 m, $\beta_2 = -8.019 \times 10^{-2}$ ps^2·km^{-1}, $\beta_3 = 2.881 \times 10^{-2}$ ps^3·km^{-1}, $\beta_4 = -1.852 \times 10^{-4}$ ps^4·km^{-1}, $P_1 = 1$ mW, $P_2 = 1$ mW, $\gamma = 122.7$ W^{-1}·km^{-1}, $\lambda_1 = 1522$ nm, and $\lambda_2 = 1618$ nm.

A gain of 50.59 dB and 55 nm gain bandwidth were realized in the two-sideband model in Figure 5.

While using the four-sideband theory, a gain and gain bandwidth of 50.59 dB and 55 nm were realized, respectively, for a dual-pump FOPA based on the PCF.

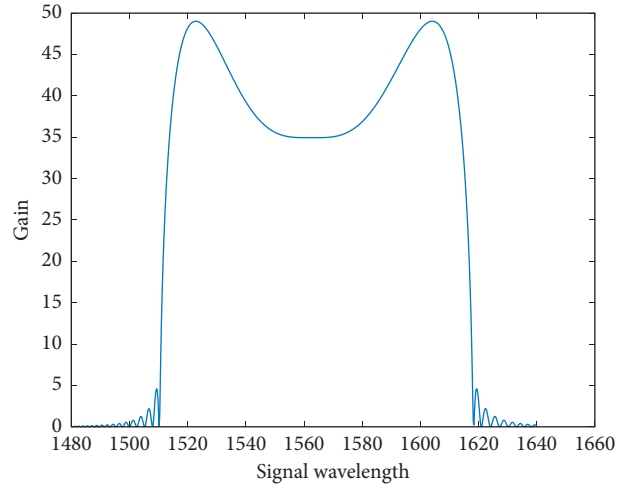

Figure 3: Simulation of a dual-pump HNLF-based FOPA gain using the two-sideband theory.

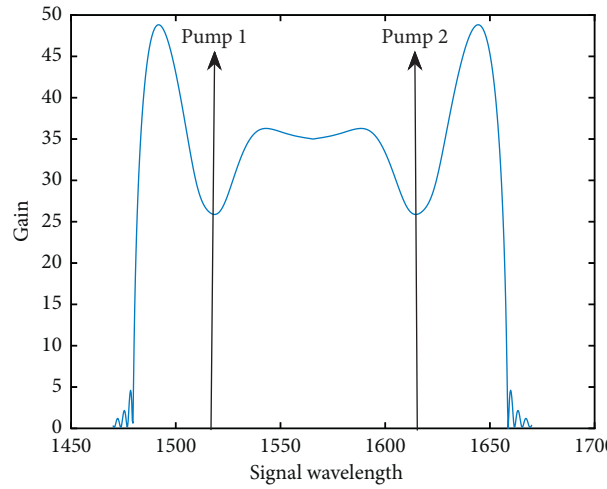

Figure 4: Simulation of a dual-pump HNLF-based FOPA gain using the four-sideband theory.

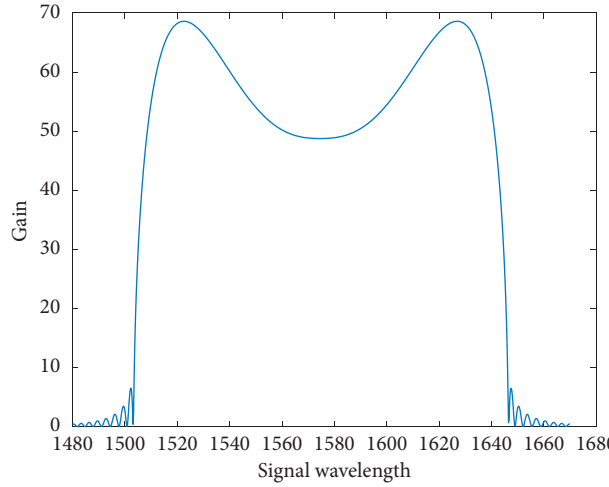

Figure 5: Simulation of a dual-pump PCF-based FOPA gain using the two-sideband theory.

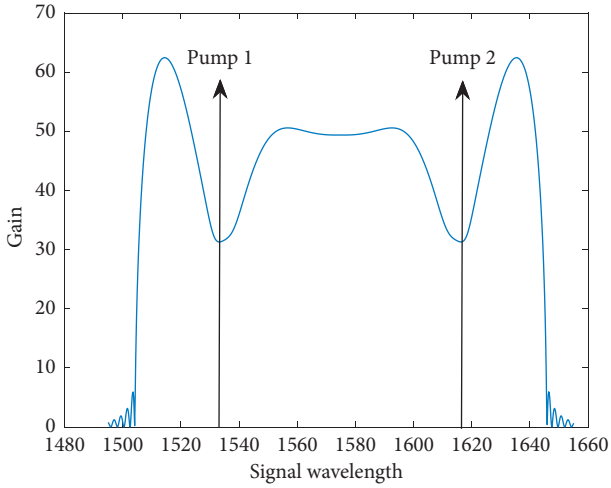

Figure 6: Simulation of a dual-pump PCF-based FOPA gain using the four-sideband theory.

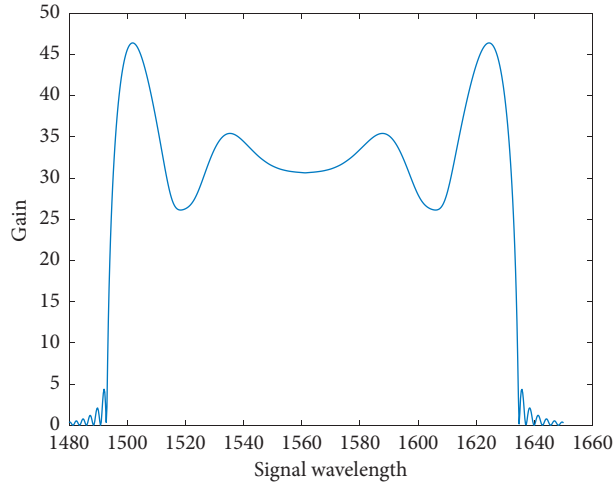

Figure 7: Simulation graph of a HNLF-based FOPA with higher third-order dispersion coefficient.

We also considered the effect of the third-order dispersion parameter on the flat gain area of the bandwidth. Considering the amplifier of Figure 7, we can show that the flat gain area is influenced by β_3. A higher value of β_3 led to gain flatness shown in Figure 7, while a lower value led to a gain shape shown in Figure 8.

The value of the third-order dispersion parameter for a fiber plays a crucial role in determining the flatness of the gain profile. Hence, it should be considered when designing FOPAs.

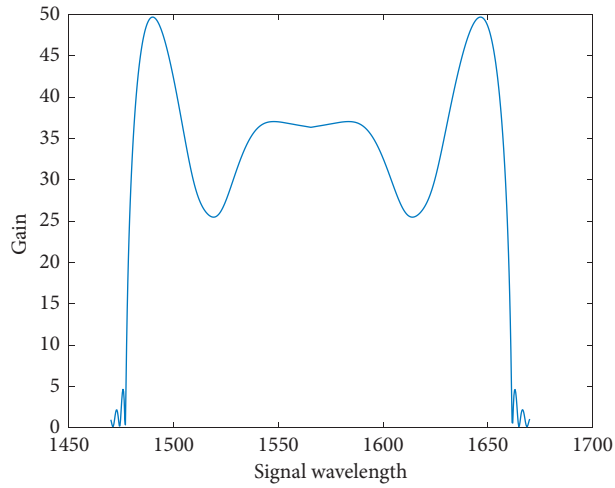

Figure 8: Simulation graph of a HNLF-based FOPA with lower third-order dispersion coefficient.

4. Discussion

A validation of the two-sideband theory and the four-sideband models has been done through the design of a dual-pump HNLF-based FOPA and a dual-pump PCF-based FOPA. A gain of 36 dB and gain bandwidth of 32 nm were obtained for the HNLF-based two-pump FOPA, while a gain of 50.59 dB and gain bandwidth of 55 nm were achieved for the PCF-based two-pump FOPA. It is observed that the four-sideband theory helps in predicting the gain shrinkage around the pumps for the amplifier allowing for a complete design picture, while the two-sideband theory does not predict the gain shrinkage. The gain shrinkage predicted in four-sideband theory is attributed to two extra FWM sidebands which are due to Bragg scattering and modulation instability and occurs just outside the flat gain area on the edges of the pumps. The analytical model put emphasis on the linear wave-vector mismatches to explain how the sideband and its closest pump interact. Dispersion parameters have a greater role in how the interaction between idlers and pump occurs, and thus modelling around them leads to a more accurate analytical technique. The model clearly gives a detailed insight into the interactions of the pump and idler closest to it through the linear wave mismatches allowing a designer to manipulate the dispersion parameters for a better design. In this model, we were able to predict the gain dips around the pumps when a signal is placed close to either of the pumps (i.e., 10 nm). In [12], we noted that our gain curves were comparable to the practical gain curves as discussed in Section 6.2 of their article. Similarly, in [11], the theoretical, numerical, and practical FOPAs were designed and the gain curves were compared, and it was observed that the curves differed greatly around the pumps, with the numerical and practical designs predicting the dips around the pumps. An offhand analysis of the curves we obtained using the four-sideband model indicates that they are far comparable to the practical and numerical gain curves obtained in [10–12]. Thus, these experimental results in the literature agree with our analytical results and support our claim that the four-sideband model is a possible option for FOPA design especially when the signal wavelength is close to the pump wavelength. It is also a model that can be easily used by any new FOPA designer as it is easy to follow and implement. An analysis of the third-order dispersion parameter was also done, and it was observed that it tends to distort the gain spectrum around the ZDW, and this is mainly due to rapid phase

mismatches that arise because of unavoidable phase modulation between the pumps. It is thus important to consider the third-order dispersion parameter when choosing a fiber for use in designing FOPA. Compared to the other theoretical models, we found ours better, as it set to reproduce exactly what the practical and numerical techniques achieve, but it still has room for further improvement by taking into consideration the pump depletion, gain saturation, and fiber losses.

5. Conclusions

Theoretical models of the two-sideband and four-sideband models have been developed and validated by designing a dual-pump HNLF-based FOPA and a dual-pump PCF-based FOPA. A gain of 36 dB and gain bandwidth of 32 nm were obtained for the HNLF-based two-pump FOPA, while a gain of 50.59 dB and gain bandwidth of 55 nm were achieved for the PCF-based two-pump FOPA. It is observed that the four-sideband theory helps in predicting the gain shrinkage around the pumps for the amplifier allowing for a complete design picture, while the two-sideband theory does not predict the gain shrinkage. A study of the third-order dispersion has shown that it has an adverse effect on the gain flatness.

Data Availability

The data used to support the findings of this study are available from the corresponding author upon request.

Conflicts of Interest

The authors declare that they have no conflicts of interest.

Acknowledgments

This research was funded by Pan African University.

References

[1] M. Jazayerifar, S. Warm, R. Elschner et al., "Performance evaluation of DWDM communication systems with fiber optical parametric amplifiers," *Journal of Lightwave Technology*, vol. 31, no. 9, pp. 1454–1461, 2013.

[2] I. Sackey, R. Elschner, M. Nölle et al., "Characterization of a fiber-optical parametric amplifier in a 5 × 28-GBd 16-QAM DWDM system," in *Proceedings of the Optical Fiber Communication Conference (OFC 2014)*, pp. 1–3, San Francisco, CA, USA, March 2014.

[3] A. Vedadi, E. Lantz, H. Maillotte, and T. Sylvestre, "Gain oscillations in two-pump fiber optical parametric amplifiers," in *Proceedings of the 2008 IEEE/LEOS Winter Topical Meeting Series*, pp. 65-66, Sorrento, Italy, January 2008.

[4] M. A. Shoaie, A. Mohajerin-Ariaei, A. Vedadi, and C.-S. Brès, "Wideband generation of pulses in dual-pump optical parametric amplifier: theory and experiment," *Optics Express*, vol. 22, no. 4, pp. 4606–4619, 2014.

[5] M.-C. Min-Chen Ho, M. E. Marhic, K. Y. K. Wong, and L. G. Kazovsky, "Narrow-linewidth idler generation in fiber four-wave mixing and parametric amplification by dithering two pumps in opposition of phase," *Journal of Lightwave Technology*, vol. 20, no. 3, pp. 469–476, 2002.

[6] A. Vedadi, M. E. Marhic, E. Lantz, H. Maillotte, and T. Sylvestre, "Investigation of gain ripple in two-pump fiber optical parametric amplifiers," *Optics Letters*, vol. 33, no. 19, pp. 2203–2205, 2008.

[7] N. Cao, H. Zhu, P. Li et al., "Flat and ultra-broadband two-pump fiber optical parametric amplifiers based on photonic crystal fibers," *Optical Review*, vol. 25, no. 3, pp. 316–322, 2018.

[8] C. J. McKinstrie and S. Radic, "Parametric amplifiers driven by two pump waves with dissimilar frequencies," *Optics Letters*, vol. 27, no. 13, pp. 1138–1140, 2002.

[9] S. Radic and C. J. McKinstrie, "Two-pump fiber parametric amplifiers," *Optical Fiber Technology*, vol. 9, no. 1, pp. 7–23, 2003.

[10] T. Richter, B. Corcoran, S. L. Olsson et al., "Experimental characterization of a phase-sensitive four-mode fiber-optic parametric amplifier," in *Proceedings of the 2012 38th European Conference and Exhibition on Optical Communications*, pp. 1–3, Amsterdam, Netherlands, September 2012.

[11] A. Bogris, D. Syvridis, P. Kylemark, and P. A. Andrekson, "Noise characteristics of dual-pump fiber-optic parametric amplifiers," *Journal of Lightwave Technology*, vol. 23, no. 9, pp. 2788–2795, 2005.

[12] J. M. Chavez Boggio, J. D. Marconi, S. R. Bickham, and H. L. Fragnito, "Spectrally flat and broadband double-pumped fiber optical parametric amplifiers," *Optics Express*, vol. 15, no. 9, pp. 5288–5309, 2007.

[13] M. Taghizadeh, M. Hatami, H. Pakarzadeh, and M. K. Tavassoly, "Pulsed optical parametric amplification based on photonic crystal fibres," *Journal of Modern Optics*, vol. 64, no. 4, pp. 357–365, 2017.

[14] M. E. Marhic, *Fiber Optical Parametric Amplifiers Oscillators and Related Devices*, Cambridge University Press, Cambridge, UK, 2007.